Steel and Composite Structures, *Vol. 28, No. 2 (2018) 195-207*
DOI: https://doi.org/10.12989/scs.2018.28.2.195

Reliability analysis-based conjugate map of beams reinforced by ZnO nanoparticles using sinusoidal shear deformation theory

Behrooz Keshtegar [*1] and Reza Kolahchi [2]

[1] *Department of Civil Engineering, Faculty of Engineering, University of Zabol, P.B. 9861335-856, Zabol, Iran*
[2] *Department of Civil Engineering, Meymeh Branch, Islamic Azad University, Meymeh, Iran*

(*Received October 7, 2017, Revised March 4, 2018, Accepted May 17, 2018*)

Abstract. First-order reliability method (FORM) is enhanced based on the search direction using relaxed conjugate reliability (RCR) approach for the embedded nanocomposite beam under buckling failure mode. The RCR method is formulated using discrete conjugate map with a limited scalar factor. A dynamical relaxed factor is proposed to control instability of proposed RCR, which is adjusted using sufficient descent condition. The characteristic of equivalent materials for nanocomposite beam are obtained by micro-electro-mechanical model. The probabilistic model of nanocomposite beam is simulated using the sinusoidal shear deformation theory (SSDT). The beam is subjected to external applied voltage in thickness direction and the surrounding elastic medium is modeled by Pasternak foundation. The governing equations are derived in terms of energy method and Hamilton's principal. Using exact solution, the implicit buckling limit state function of nanocomposite beam is proposed, which is involved various random variables including thickness of beam, length of beam, spring constant of foundation, shear constant of foundation, applied voltage, and volume fraction of ZnO nanoparticles in polymer. The robustness, accuracy and efficiency of proposed RCR method are evaluated for this engineering structural reliability problem. The results demonstrate that proposed RCR method is more accurate and robust than the excising reliability methods-based FORM. The volume fraction of ZnO nanoparticles and the applied voltage are the sensitive variables on the reliable levels of the nanocomposite beams.

Keywords: reliability analysis; nanocomposite beam; buckling force; relaxed conjugate reliability method

1. Introduction

Nanocomposite particles are widely applied to use in numerous fields of engineering including civil, aeronautical, architectural, aerospace, and mechanical engineering. The addition of nanoparticles in the structural components can be improved the thermal, electrical, and mechanical properties of structures. These structures are subjected to different statical and dynamical loads. However, the reliability analysis of nanocomposite structures is an important issue to evaluate the reliable construction of the enhanced structural components.

Mechanical analysis of nanocomposite structures including the beam, plate and shell are investigated by many authors. Wuite and Adali (2005) presented a multiscale analysis for reinforced polymer composite beams by carbon nanotube (CNT). The pure bending and bending-induced local buckling of reinforced single-walled carbon nanotube (SWCNT) nanocomposite beam was investigated by Vodenitcharova and Zhang (2006). Shen (2009) investigated the nonlinear bending of a simply supported functionally graded nanocomposite plates reinforced by SWCNTs in thermal environments. Thermal buckling and postbuckling behavior of functionally graded nanocomposite plates by Shen and Zhang (2010). Wattanasakulpong and Ungbhakorn (2013) studied the bending, vibration and buckling behaviors of carbon nanotube reinforced composite beams under the Pasternak elastic foundation with Winkler and shear springs. Distortional buckling of a steel-concrete composite box beam was investigated under a negative moment by Zhou *et al*. (2015). An investigation on the nonlinear dynamic response and vibration of the imperfect laminated three-phase polymer nanocomposite panel resting on elastic foundations was presented by Duc *et al*. (2015). The biaxially buckling and postbuckling behaviors of reinforced multilayer nanocomposite plates with graphene nanoplatelets are studied by Song *et al*. (2017) using first-order shear deformation plate theory. The bending, buckling and free vibration analysis of SWCNTs on elastic foundation was studied using the shear deformation effect by Tagrara *et al*. (2015). Nonlocal nonlinear buckling analysis of polymeric temperature-dependent microplates resting on an elastic foundation was investigated by Kolahchi *et al*. (2015). Van Thu and Duc (2016) presented an analytical approach to investigate the non-linear dynamic response and vibration of an imperfect three-phase laminated nanocomposite cylindrical panel resting on elastic foundations in thermal environments. Buckling of pipe reinforced by armchair double walled boron nitride nanotubes (DWBNNTs) was investigated by Mosharrafian and Kolahchi (2016). Duc *et al*. (2017a, b, c) studied

∗Corresponding author, Ph.D.,
E-mail: bkeshtegar@uoz.ac.ir

http://www.techno-press.org/?journal=scs&subpage=6
ISSN: 1229-9367 (Print), 1598-6233 (Online)

thermal and mechanical stability of a functionally graded composite truncated conical shell, plates and double curved shallow shells reinforced by carbon nanotube fibers. Based on Reddy's third-order shear deformation plate theory, the nonlinear dynamic response and vibration of imperfect functionally graded carbon nanotube-reinforced composite plates was analyzed by Thanh *et al*. (2017). Duc *et al*. (2018) presented the first analytical approach to investigate the nonlinear dynamic response and vibration of imperfect rectangular nanocompsite multilayer organic solar cell subjected to mechanical loads using the classical plate theory.

To the best of our knowledge, no investigation has been performed on the reliability analysis of nanocomposite beams reinforced by ZnO nanoparticles. Generally, the Monte Carlo Simulation (MCS) Echard *et al*. 2011, dimension reduce method (Lee *et al*. 2008), the sequential sampling approaches (Lee and Jung 2008, Zhuang and Pan 2012, Jia *et al*. 2016) (e.g., Kriging (Dubourg *et al*. 2011, Echard *et al*. 2013), adaptive Kriging (Echard *et al*. 2011), response surface method (Liu and Moses 1994, Goswami *et al*. 2016), support vector machine (Alibrandi *et al*. 2015, neural network Chojaczyk *et al*. 2015), polynomial chaos expansion (Hu and Youn 2011) and the M5Tree (Keshtegar and Kisi 2017), moment methods (Zhao and Ono 2001, Zhao and Lu 2007, Lu *et al*. 2017), first-order reliability method (FORM) (Hasofer and Lind 1974, Rackwitz and Flessler 1978, Yang 2010, Gong and Yi 2011, Bonstrom and Corotis 2014, Keshtegar and Meng 2017, Keshtegar 2018a, b) and the second-order reliability method (Der Kiureghian and Dakessian 1998) are applied for structural reliability analysis. The MCS is computationally inefficient scheme to evaluate the failure probability compare to FORM due to require large data samples for evaluating the buckling force using implicit performance function of nanostructural problems. Commonly, the iterative FORM- based Hasofer and Lind (1974)-Rackwitz and Flessler (1978) (HL-RF) is applied to estimate the structural failure probabilities reliability. The HL-RF formula may produce the numerical instability as chaotic and periodic solutions for nonlinear engineering problems (Yang 2010, Keshtegar 2016, Keshtegar and Bagheri 2018). Several modified algorithms were proposed to enhance the numerical instabilities of FORM using the steepest descent search direction including stability transformation method (STM) (Yang 2010, Meng *et al*. 2017), improved HL-RF (*i*HL-RF) (Liu and Der Kiureghian 1991), finite -step length (FSL) (Gong and Yi 2011), finite-step length-based Armijo (Keshtegar and Chakraborty 2018a), and relaxed HL-RF (Keshtegar and Meng 2017). Lu *et al*. (2015) used the FORM for evaluating the safety level of square columns designed by AISC and Eurocode 4. The failure probabilities of stainless steel joint design according to Eurocodes were evaluated using FORM based on the nonlinear finite element model by Averseng *et al*. (2017). Keshtegar (2016, 2017, 2018a, b) showed that the conjugate search direction can be improved the robustness of reliability analysis using Armijo rules (Keshtegar 2017, El Amine Ben Seghie *et al*. 2018) and sufficient descent condition (Keshtegar 2016, Keshtegar and Kisi 2017, Keshtegar and Chakraborty 2018b). Thus, the accuracy, robustness and efficiency of the FORM are three important issues for reliability analysis of a noncomposite beam under implicit buckling performance function.

The aim of this study is to present a novel FORM formula-based conjugate search direction for reliability analysis of sinusoidal beams reinforced by ZnO nanoparticles subjected to external applied voltage. The different uncertainties including geometry, applied external voltage, the stiffness of the foundation, volume fraction of nanoparticles is considered based on an implicit theoretical probabilistic model, which is developed based on SSDT for buckling loads of the nanocomposite beam. The efficiency, robustness and accuracy of FORM formula are improved using relaxed conjugate reliability (RCR) method. The proposed RCR is compared with several existing reliability methods including HL-RF, improved HL-RF (Liu and Der Kiureghian 1991), FSL (Gong and Yi 2011), STM (Yang 2010), and conjugate HL-RF (Keshtegar and Miri 2014). Results demonstrate that the proposed RCR method has a good manner for both robustness and accuracy compared to existing FORM formulas. The negative voltage and the increasing the volume fraction of ZnO nanoparticles can be improved the reliable levels of nanocomposite beams.

2. Reliability analysis-based relaxed conjugate approach

The failure probability is estimated by the below multi-dimensional integral (Keshtegar and Bagheri 2018)

$$P_f = \int_{g(\boldsymbol{X})\le 0}\!\!\ldots\int f_{\boldsymbol{X}}(x_1,\ldots,x_n)dx_1..dx_n \tag{1}$$

where, $g(X)$ represents the limit state function (LSF), which is can be computed using a probabilistic buckling model of a nanocomposite beam based on random variables $X = (x_1, x_2,..., x_n)^T$. f_X is the joint probability density function (PDF) for X.

The P_f using FORM is approximated using reliability index (β) as $P_f \approx \Phi(-\beta)$. The iterative FORM formula is developed using the relaxed approach based on the conjugate search direction to estimate the reliability index as follows

$$\boldsymbol{U}_{k+1} = \xi_k \boldsymbol{U}^c_{k+1} + (1-\xi_k)\boldsymbol{U}_k \tag{2}$$

where

$$\boldsymbol{U}^c_{k+1} = \beta_{k+1}\boldsymbol{\alpha}^c_{k+1} \tag{3}$$

$$\beta_{k+1} = \frac{\nabla^T g(\boldsymbol{U}_k)\boldsymbol{U}_k - g(\boldsymbol{U}_k)}{\nabla^T g(\boldsymbol{U}_k)\boldsymbol{\alpha}^c_{k+1}} \tag{4}$$

where, U^c_{k+1} the conjugate discrete direction map, which is obtained based on the normalized conjugate search direction (α^c_{k+1}), ξ_k is the relaxed factor, and $\nabla g(U_k)$ is the gradient vector of the LSF at point U_k. U_k is determined as follows (Keshtegar 2018a, 2016)

$$\boldsymbol{U}_k = \frac{\boldsymbol{X}_k - \mu_x^e}{\sigma_x^e} \tag{5}$$

where

$$\sigma_x^e = \frac{1}{f_X(\boldsymbol{X}_k)}\phi[\Phi^{-1}\{F_X(\boldsymbol{X}_k)\}] \tag{6}$$

$$\mu_x^e = \boldsymbol{X}_k - \sigma_x^e\Phi^{-1}[F_X(\boldsymbol{X}_k)] \tag{7}$$

In which, σ_x^e and μ_x^e are respectively the equivalent standard deviations and means of the X. $f_X(X_k)$ and $F_X(X_k)$ are the PDF and cumulative distribution function (CDF) at X_k, respectively. Φ^{-1} is the inverse standard normal CDF and ϕ is the standard normal PDF.

The normalized conjugate search direction (α_{k+1}^c) and relaxed factor ξ_k are two major differences between the RCR method and modified versions of conjugate FORM (Keshtegar 2016, Keshtegar 2018a, b; Keshtegar and Kisi 2017) where, α_{k+1}^c is given as follows

$$\boldsymbol{\alpha}_{k+1}^c = \frac{\boldsymbol{U}_k + \boldsymbol{d}_k}{\left\|\boldsymbol{U}_k + \boldsymbol{d}_k\right\|} \tag{8}$$

where d_k is conjugate search direction vector, which is computed as follows

$$\boldsymbol{d}_k = -\nabla g(\boldsymbol{U}_k) + \theta_k \boldsymbol{d}_{k-1} \tag{9}$$

where, θ_k is conjugate scalar factor, which is obtained as follows

$$\theta_k = \min\left\{0.95\frac{\left\|\nabla g(\boldsymbol{U}_k)\right\|^2}{\left\|\nabla g(\boldsymbol{U}_{k-1})\right\|^2}, 2\right\} \tag{10}$$

It can be concluded from Eq. (10) that $\theta_k = 0.95\frac{\|\nabla g(U_k)\|^2}{\|\nabla g(U_{k-1})\|^2} \leq 2$. Therefore, the RCR method may enhance the computational burden of FORM formula in compression with existing conjugate FORM approach without limited factor as well as the CHL-RF (Keshtegar and Miri 2014). The proposed conjugate search direction is similar to CHL-RF, when the limited factor 2 and coefficient 0.95 are neglected in θ_k using Eq. (10), thus it may be computed a large value for conjugate scalar factor as $\theta_k >> 1$. Consequently, the computational efforts of the RCR may increase to achieve the stabilization. The search direction is sensitive to the steepest descent search direction ($\nabla g(U)$), when the conjugate scalar factor is selected a small value i.e., $\theta_k << 1$, thus it may provide unstable results as well as HL-RF method. Therefore, the conjugate scalar factor $\left(\theta_k = 0.95\frac{\|\nabla g(U_k)\|^2}{\|\nabla g(U_{k-1})\|^2}\right)$ is limited to 2 due to improve its efficiency and to increase the effect of previous conjugate search direction (d_{k-1}) for controlling the instability of FORM.

Lemma: It is supposed that the d_k which is adapted using θ_k in Eq. (10) holds the sufficient descent condition as $\nabla^T g(U_k)d_k < -c_1\|\nabla g(U_k)\|^2$ in which $0 < c_1 < 1$, thus $U_k = U_{k+1}$ for $k \to \infty$

Proof: For $k = 0$, we have $d_0 = -\nabla g(U_0)$ thus $-\|\nabla g(U_k)\|^2 < -c_1\|\nabla g(U_k)\|^2$ based on the sufficient descent condition. It can be conducted that $\theta_k = 0.95\frac{\|\nabla g(U_k)\|^2}{\|\nabla g(U_{k-1})\|^2}$ based on Eq. (10), thus by combining Eqs. (9) and (10), it is obtained

$$\nabla^T g(\boldsymbol{U}_k)\boldsymbol{d}_k = -\left\|\nabla g(\boldsymbol{U}_k)\right\|^2 + \theta_k \nabla^T g(\boldsymbol{U}_k)\boldsymbol{d}_{k-1} \tag{11}$$

It can be rewritten the Eq. (11) based on condition $\theta_k = \frac{\|\nabla g(U_k)\|^2}{\|\nabla g(U_{k-1})\|^2}$ as follows

$$\begin{aligned}\nabla^T g(\boldsymbol{U}_k)\boldsymbol{d}_k &< -\left\|\nabla g(\boldsymbol{U}_k)\right\|^2 \\ &+ \frac{\left\|\nabla g(\boldsymbol{U}_k)\right\|^2}{\left\|\nabla g(\boldsymbol{U}_{k-1})\right\|^2}\nabla^T g(\boldsymbol{U}_k)\boldsymbol{d}_{k-1} < -\left\|\nabla g(\boldsymbol{U}_k)\right\|^2\end{aligned} \tag{12}$$

It can be concluded that the sufficient descent condition based on Eq. (10) can be satisfied in the proposed RCR formula, theoretically.

The relaxed factor in the RCR method is important factor as well as the conjugate search direction. The relaxed factor is defined as follows

$$\xi_k = \begin{cases} \delta\frac{\left\|\boldsymbol{U}_k - \boldsymbol{U}_{k-1}\right\|}{\left\|\boldsymbol{U}_{k+1}^c - \boldsymbol{U}_k\right\|}\xi_{k-1} & \left\|\boldsymbol{U}_{k+1}^c - \boldsymbol{U}_k\right\| \geq \left\|\boldsymbol{U}_k - \boldsymbol{U}_{k-1}\right\| \\ \xi_{k-1} & \left\|\boldsymbol{U}_{k+1}^c - \boldsymbol{U}_k\right\| < \left\|\boldsymbol{U}_k - \boldsymbol{U}_{k-1}\right\| \end{cases} \tag{13}$$

Where, δ is the adjusting factor that it can be given as $0.9 \leq \delta < 1$. The relaxed factor can be slightly increased when a small adjusting factor is selected, thus the convergence rate of the RCR method my increase for highly nonlinear reliability problems. As seen from the proposed relaxed factor, the relaxed factor $\xi_k \leq \xi_{k-1}$ and $\xi_0 = 1$; thus, $0 \leq \xi_k \leq 1$. If $\left\|\boldsymbol{U}_{k+1}^c - \boldsymbol{U}_k\right\| \geq \left\|\boldsymbol{U}_k - \boldsymbol{U}_{k-1}\right\|$, then $0 < \frac{\left\|\boldsymbol{U}_k - \boldsymbol{U}_{k-1}\right\|}{\left\|\boldsymbol{U}_{k+1}^c - \boldsymbol{U}_k\right\|} \leq 1$ thus, we have $0 \leq \xi_k \leq \xi_{k-1}$. It can be concluded that $\lim_{k\to\infty}\xi_k = 0$ for $0 \leq \xi_k \leq \xi_{k-1}$. This means that the new and previous points are located on a same directions, thus it is captured a fixed point for $k \to \infty$ i.e., $U_{k+1} = U_k$.

In addition, the proposed relaxed factor based on Eq. (13) is established based on the sufficient descent criterion $\left\|\boldsymbol{U}_{k+1}^c - \boldsymbol{U}_k\right\| < \left\|\boldsymbol{U}_k - \boldsymbol{U}_{k-1}\right\|$. We will have

$$\begin{aligned}&\left\|\boldsymbol{U}_3-\boldsymbol{U}_2\right\|=c_1\left\|\boldsymbol{U}_2-\boldsymbol{U}_1\right\|,\\ &\left\|\boldsymbol{U}_4-\boldsymbol{U}_3\right\|=c_1c_2\left\|\boldsymbol{U}_2-\boldsymbol{U}_1\right\|,\ldots,\\ &\left\|\boldsymbol{U}^c_{k+1}-\boldsymbol{U}_k\right\|=\left\|\boldsymbol{U}_2-\boldsymbol{U}_1\right\|\prod_{i=1}^{k-1}c_i,\quad 0\le c_i<1\end{aligned}\tag{14}$$

For $k \rightarrow \infty$, $\lim_{k\to\infty}\prod_{i=1}^{k-1}c_i=0$, $0\le c_i<1$ thus, it can be obtained $\left\|\boldsymbol{U}^c_{k+1}-\boldsymbol{U}_k\right\|=0$ when $\left\|\boldsymbol{U}^c_{k+1}-\boldsymbol{U}_k\right\|<\left\|\boldsymbol{U}_k-\boldsymbol{U}_{k-1}\right\|$. This means that the proposed relaxed approach-based conjugate search direction can improve the robustness of FORM formula.

Based on the above relations; the iterative formula of RCR method can be applied in a computer code by the following steps:

1. Define the limit state function $g = 0$ for the nanocomposite beam under buckling failure mode
2. Give the statistical properties of random variables as means μ, standard deviations σ and probability distribution functions
3. Give the parameters of the RCR method as $\varepsilon << 1$ (stopping criterion), Let $k = 0$, and the set the initial point $X_0 = \mu$, $d_0 = 0$, δ, and $\xi_0 = 1$.
4. Transfer the random variable from X-space into U-space based on Eqs. (5)-(7).
5. Compute $\nabla g(U_k)$ and LSF at point U_k.
6. Compute the θ_k using Eq. (10) and d_k using Eq. (9)
7. Determine normalized conjugate search direction vector α^c_{k+1} based on Eq. (8) using the results obtained in Step 6.
8. Compute the reliability index (β_{k+1}) using Eq. (4).
9. Compute point U^c_{k+1} in terms of the proposed conjugate discrete map in Eq. (3).
10. Adopt the relaxed factor ξ_k in terms of Eq. (13).
11. Determine the new point based on the proposed conjugate search direction-based relaxed approach in Eq. (2).
12. Compute $X_{k+1} = \mu + \sigma U_{k+1}$.
13. If $\|U_{k+1} - U_k\| < \varepsilon$ then stop, else $k = k + 1$ and **Go to Step 4**.

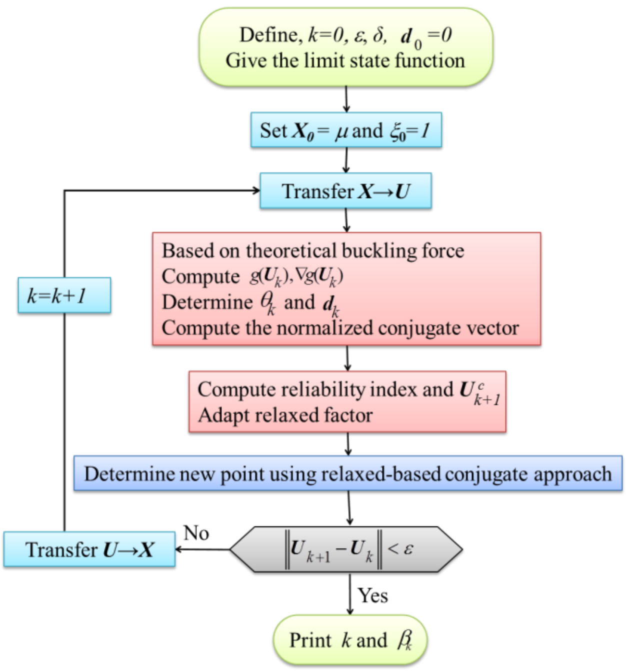

Fig. 1 Framework of the RCR method for reliability analysis of nanocomposite beams

Based on the above steps, the framework of the RCR method is plotted in Fig. 1 for reliability analysis of the nanocomposite beams under buckling forces. Unlike the steepest descent search direction in FORM formula of the HL-RF (Hasofer and Lind 1974, Rackwitz and Flessler 1978), STM (Yang 2010), and improved HL-RF (Liu and Der Kiureghian 1991) methods, the new conjugate search direction is not located along the pervious steepest descent search direction vectors. As mentioned, theinstability of the FORM formula–based proposed relaxed conjugate reliability method can be controlled by the adaptive relaxed factor in Eq. (13) at each iteration. A smaller relaxed factor may be computed at final iterations for highly nonlinear LSFs due to $\xi_k < \xi_{k-1}$. Consequently, the spectral radius of the Jacobian matrix ($\rho(\bar{J})$) can be enriched based on the RCR method by the enhanced Jacobian matrix as $[\bar{\boldsymbol{J}}]=\boldsymbol{I}+\xi_k([\boldsymbol{J}]-\boldsymbol{I})\left([\boldsymbol{J}]=\frac{\boldsymbol{U}^c_{k+1}}{\partial u_j}|_{\boldsymbol{U}_k}\right)$. Therefore, the RCR can improve the instability of FORM, theoretically. In addition, for $k \rightarrow \infty$, $\xi_k = 0$ thus $[\bar{\boldsymbol{J}}]_k=\boldsymbol{I}$ and $\rho(\bar{\boldsymbol{J}})=1$. This means that the proposed RCR method provides a fixed point.

The conjugate scalar factor in Eq. (10) is scaled by factor 0.95 to satisfy the sufficient descent condition, while the conjugate scalar factor in chaotic conjugate stabilitytransformation method Keshtegar 2016, limited conjugate gradient (Keshtegar 2017), chaotic chaos control (Keshtegar 2016) and hybrid conjugate gradient (Keshtegar and Kisi 2017; Keshtegar and Chakraborty 2018b) methods is given as $\frac{\left\|\nabla g(\boldsymbol{U}_k)\right\|^2}{\left\|\nabla g(\boldsymbol{U}_{k-1})\right\|^2}$. The finite step size with Armijo rule (Keshtegar 2016, Keshtegar and Kisi 2017, Keshtegar and Chakraborty 2018b) and a chaotic control factor (Keshtegar 2016, 2017) are used to control instability of existing FORM formulas-based RCR formula. The adjusted relaxed factor is major difference of the RCR method compared to existing conjugate FORM. A completed formulation is developed for RCR as well as other adaptive conjugate FORMs (e.g., El Amine Ben Seghier *et al*. 2018, Keshtegar 2017, 2018a, Keshtegar and Chakraborty 2018b, Keshtegar and Bagheri 2018) to satisfy the sufficient decent condition.Therefore, the new formulation of conjugate FORM is established based on the complicated iterative formula compared to the existing FORM algorithms-based steepest descent search direction such as STM (Yang 2010), directional STM(Meng *et al*. 2017), relaxed HL-RF (Keshtegar and Meng 2017) and finite-step length methods (Gong and Yi 2011, Keshtegar and Chakraborty 2018a). However, the improved formulas of FORM using steepest descent search direction and conjugate sensitivity vector my inaccurately provide the most probable point for some nonlinear reliability problems with several points from LSF which are located on beta-cycle hypersphere with same distance from origin in normal standard space.

3. Mathematical modeling of structure

As shown in Fig. 2, a polymeric beam with the length of L and cross section of $b\times h$ is reinforced uniformly with piezoelectric ZnO nanoparticles. The structure is subjected to external applied voltage in thickness direction and surrounded by elastic foundation.

The structure is modeled with SSDT where the displacement field based on this theory can be written as follows (Thai and Vo 2012, Li *et al*. 2017)

$$u_1(x,z,t)=u(x,t)-z\frac{\partial w(x,t)}{\partial x}+f\psi(x,t)\ , \tag{15}$$

$$u_2(x,z,t)=0\ , \tag{16}$$

$$u_3(x,z,t)=w(x,t)\ , \tag{17}$$

where u_1, u_2, and u_3 are the displacement of the mid plane in the axial, transverse and thickness directions; ψ represents the rotation of cross section about y axis; $f=\frac{h}{\pi}sin\left(\frac{\pi z}{h}\right)$. Using Eqs. (15) to (17), the nonlinear strain-displacement relations using Von-Karman theory are as follows

$$\varepsilon_{xx}=\frac{\partial u}{\partial x}-z\frac{\partial^2 w}{\partial x^2}+\frac{1}{2}\left(\frac{\partial w}{\partial x}\right)^2+f\frac{\partial\psi}{\partial x}, \tag{18}$$

$$\varepsilon_{xz}=\cos\left(\frac{\pi z}{h}\right)\psi. \tag{19}$$

Since the ZnO nanoparticles are piezoelectric, however, the stress (σ) and the strain (ε) from the mechanical side with an electrical displacement (D) and electric field (E) from the electrostatic side can be coupled. The electric field (E_k) based on electric potential is defined as follows (Barzoki *et al*. 2012)

$$E_k=-\nabla\Phi. \tag{20}$$

The electric potential distribution is considered as follow (Kolahchi *et al*. 2016, Yang and Yu 2017)

$$\Phi(x,z,t)=-\cos\left(\frac{\pi z}{h}\right)\phi(x,t)+\frac{2V_0 z}{h}, \tag{21}$$

where V_0 is the external voltage. According to the SSDT, electromechanical coupling relationship can be summarized as below

$$\sigma_{xx}=Q_{11}\varepsilon_{xx}+e_{31}\left(\frac{\pi}{h}\sin\left(\frac{\pi z}{h}\right)\phi+\frac{2V_0}{h}\right). \tag{22}$$

$$\sigma_{xz}=Q_{55}\varepsilon_{xz}-e_{15}\left(\cos\left(\frac{\pi z}{h}\right)\frac{\partial\phi}{\partial x}\right), \tag{23}$$

$$D_x=e_{15}\varepsilon_{xz}+\in_{11}\left(\cos\left(\frac{\pi z}{h}\right)\frac{\partial\phi}{\partial x}\right), \tag{24}$$

$$D_z=e_{31}\varepsilon_{xx}-\in_{33}\left(\frac{\pi}{h}\sin\left(\frac{\pi z}{h}\right)\phi+\frac{2V_0}{h}\right), \tag{25}$$

where Q_{ij}, e_{ij} and $\in_{ij}$ are elastic, piezoelectric and dielectric constants, respectively. Noted that the using the micro-electro-mechanical model the mechanical and electrical properties of the structure can be obtained by (Tang and Tong 2001). Based on energy method and Hamilton's principal, the governing equations can be given as follows

$$\delta u:\frac{\partial^2 u}{\partial x^2}+\frac{\partial w}{\partial x}\frac{\partial^2 w}{\partial x^2}=0, \tag{26}$$

$$\begin{aligned}\delta w:&-Q_{11}I\frac{\partial^4 w}{\partial x^4}+\frac{24Q_{11}I}{\pi^3}\frac{\partial^3\psi}{\partial x^3}\\&-\left(2e_{31}V_0+N_x^M\right)\frac{\partial^2 w}{\partial x^2}-k_w w+k_g\nabla^2 w=0,\end{aligned} \tag{27}$$

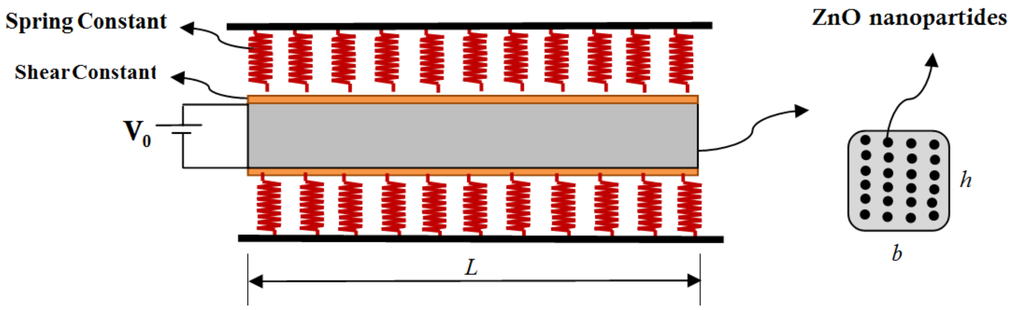

Fig. 2 The schematic view of the nanocomposite beam

$$\delta\psi : -\frac{24Q_{11}I}{\pi^3}\frac{\partial^3 w}{\partial x^3} + \frac{6Q_{11}I}{\pi^2}\frac{\partial^2\psi}{\partial x^2} + \frac{e_{31}h}{2}\frac{\partial\phi}{\partial x} - \frac{Q_{55}A}{2}\psi + \frac{e_{15}h}{2}\frac{\partial\phi}{\partial x} = 0, \tag{28}$$

$$\delta\phi : -\frac{2h}{\pi}\frac{\partial^2 w}{\partial x^2} + \frac{h}{2}\frac{\partial\psi}{\partial x} - \frac{\pi^2 \in_{33}}{2h}\phi + \frac{h}{2}\frac{\partial\psi}{\partial x} + \frac{h\in_{11}}{2}\frac{\partial^2\phi}{\partial x^2} = 0. \tag{29}$$

In the above equation, k_w and k_g are respectively the spring and shear constants of elastic medium and N_x^M is the internal applied force to the beam. Finally, using an analytical solution adopted by Tan and Tong 2001, the governing equations can be written as

$$\left([K] + P_{cr}\lfloor K_g \rfloor\right)\{d\} = 0, \tag{30}$$

In these relationships, P_{cr} is the critical buckling load. Also, $[K]$, $[K_g]$ and $[d]$ respectively, represent the stiffness matrix, geometric matrix and displacement vector. However, using eigenvalue problem, the critical buckling load (P_{cr}) of structure can be obtained.

4. Define limit state function

The failure probability i.e., $P_f \approx \Phi(-\beta)$ can be approximated based on a probabilistic model using analytical solution of nanocomposite beam. The limit state function based on the buckling force, which is theoretically obtained using Eq. (30) is given as below

$$g = P_{cr} - P \tag{31}$$

where, P is the axial compressive applied load, which is considered as 50 GPa. P_{cr} is the theoretical buckling force, which is computed using Eq. (30). This example involves six normal and non-normal basic random variables, whose statistical properties are tabulated in Table 1. It is noted that in Table 1, *rho* is the volume fraction of ZnO nanoparticles in beam.

5. Comparative and parametric results

There are coded different reliability methods by using MATLAB software. The stopping criterion ε is selected as $\varepsilon = 10^{-6}$ for all reliability FORM schemes. Based on the performance function in Eq. (31) and the random variables in Table 1, the reliability index is computed for the buckling capacity of nanocomposite beam that the gradient vector of the limit state function is computed using the finite difference approach at each iteration for FORM formulas. The material properties of polyethylene (PE) beam as well as ZnO nanoparticles are chosen from Refs. (Barzoki *et al*. 2012, Ghorbanpour *et al*. 2015).

5.1 Validation

Buckling force for beam with reinforced nanoparticles ZnO has not been studied. So to verify our results, eliminating the effects of ZnO nanoparticles (*rho* = 0), foundations ($k_w = k_g = 0$) and piezoelectric properties, buckling analysis of a beam with SSDT is discussed. Considering the material and the geometric parameters similar to Thai and Van Thu (2012), buckling load was shown for different aspect ratios of structure in Table 2. It can be conducted, the results of the current work in accordance with reference Thai and Van Thu (2012) show that the results are accurate.

5.2 Comparative performances of reliability methods

The converged reliability results of proposed RCR method with parameter $\delta = 0.95$ for the nanocomposite beam is compared to the HL-RF Hasofer and Lind 1974, Rackwitz and Flessler 1978, *i*HL-RF (its permeates is given as $c = 10^6$) (Liu and Der Kiureghian 1991), STM (parameters of $\boldsymbol{C} = \boldsymbol{I}$ and $\lambda = 0.1$) (Yang 2010), the FSL (parameters of $c = 1.4$ and $\lambda = 30$) (Gong and Yi 2011), and the CHL-RF (with dynamical finite- step size λ which is adjusted using Armijo rule and $C = 1.5$ as $\lambda = \lambda/C$) (Keshtegar and Miri 2014). The HL-RF, STM and *i*HL-RF are established using the steepest descent search direction

Table 2 Validation of present work with other published works

L/h	TBT (Thai and Vo 2012)	SSD (Thai and Vo 2012)	SSDT (present)
5	8.9509	8.9533	8.9532
10	9.6227	9.6232	9.6231
20	9.8067	9.8068	9.8068
100	9.8671	9.8671	9.8671

Table 1 Statistical properties of random variables for nanocomposite beam structure

Random variable	h (m)	L (m)	k_w (N/m^2)	k_g (N)	*rho*	V_0 (volte)
Mean	0.4	0.5	5×10^{12}	5	0.25	100
Coefficient of variation	0.1	0.1	0.12	0.12	0.1	0.2
Standard deviation	0.04	0.05	6×10^{11}	0.6	0.025	20
Distribution	Lognormal	Normal	Gumbel	Gumbel	Lognormal	Normal
Description	Thickness of beam	Length of beam	Spring constant of foundation	Shear constant of foundation	Volume fraction of ZnO	Applied voltage

$\left(\boldsymbol{\alpha}_{k+1} = -\frac{\nabla\ g(\boldsymbol{U}_k)}{\|\nabla g(\boldsymbol{U}_k)\|}\right)$ by the following iterative FORM formula:

5.2.1 HL-RF method

$$\boldsymbol{U}_{k+1}^{HL} = \frac{\nabla^T g(\boldsymbol{U}_k)\boldsymbol{U}_k - g(\boldsymbol{U}_k)}{\nabla^T g(\boldsymbol{U}_k)\boldsymbol{\alpha}_{k+1}}\boldsymbol{\alpha}_{k+1} \tag{32}$$

5.2.2 STM method

$$\boldsymbol{U}_{k+1} = \boldsymbol{U}_k + \lambda \boldsymbol{C}(\boldsymbol{U}_{k+1}^{HL} - \boldsymbol{U}_k) \tag{33}$$

5.2.3 iHL-RF method

$$\boldsymbol{U}_{k+1} = \boldsymbol{U}_k + \alpha(\boldsymbol{U}_{k+1}^{HL} - \boldsymbol{U}_k) \tag{34}$$

The step size α is controlled using the merit function (Keshtegar and Meng 2017).

5.2.4 Finite-step length method

The FSL method is formulated based on the finite steepest descent search direction as $\boldsymbol{\alpha}_{k+1} = \frac{\boldsymbol{U}_k - \lambda\nabla g(\boldsymbol{U}_k)}{\|\boldsymbol{U}_k - \lambda\nabla g(\boldsymbol{U}_k)\|}$, in which λ is the finite-step size which is adjusted as $\lambda = \lambda/c$ when $\|\boldsymbol{U}_{k+1} - \boldsymbol{U}_k\| \geq \|\boldsymbol{U}_k - \boldsymbol{U}_{k-1}\|$, where c adjusted factor.

5.2.5 Conjugate HL-RF

The conjugate formula of FORM presented in Eqs. (3) and (4) is also applied to search most probable failure point (MPP) using the CHL-RF method that its normalized conjugate search direction is computed as $\boldsymbol{\alpha}_{k+1}^c = \frac{\boldsymbol{U}_k + \lambda_k \boldsymbol{d}_k}{\|\boldsymbol{U}_k + \lambda_k \boldsymbol{d}_k\|}$, where λ can be determined using Armijo rule as follows

$$\lambda_0 \leq \frac{100}{\|\nabla g(\boldsymbol{U}_0)\|^2} \tag{35}$$

The initial step size in Eq. (35) is adjusted as $\lambda_{k+1} = \lambda_k / C$ where C = 1.5, when $\|\boldsymbol{U}_{k+1} - \boldsymbol{U}_k\| \geq \|\boldsymbol{U}_k - \boldsymbol{U}_{k-1}\|$. The conjugate vector is computed as follows

$$\boldsymbol{d}_k = -\nabla g(\boldsymbol{U}_k) + \frac{\|\nabla g(\boldsymbol{U}_k)\|^2}{\|\nabla g(\boldsymbol{U}_{k-1})\|^2}\boldsymbol{d}_{k-1} \tag{36}$$

Two nonlinear structural problems are given to illustrate the convergence performances of FORM formulas with stopping criterion i.e., $\varepsilon = 10^{-6}$ as below:

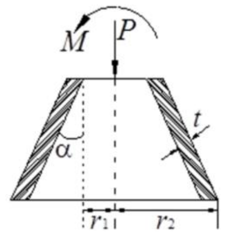

Fig. 3 The conical structure

Table 3 Random variables for conical structure

Variables	Description	Distribution	Mean	CoV
E	Young's modulus (MPa)	Lognormal	70000	0.05
t	Thickness(m)	Normal	0.0025	0.05
α	Slop angle (rad)	Normal	0.524	0.02
r_1	Internal radius(m)	Normal	0.9	0.025
M	Bending moment(N-m)	Gumbel	80000	0.08
P	Axial load(N)	Gumbel	70000	0.08

***Example 1**: A conical structure*

A conical structure as showed in Fig. 3 is considered by the following performance function (Keshtegar and Chakraborty 2018a)

$$g = 1 - \frac{1.6523}{\pi E t^2 \cos^2\alpha} \times (\frac{P}{0.66} + \frac{M}{0.41 r_1}) \tag{37}$$

This problem involves six random variables aspresented in Table 3.

***Example 2**: 24-bar space truss structure*

A high-dimensional applicable engineering reliability problem as showed in Fig. 4 with 24-truss element, 12-node, 7- gravity load (P_1 – P_7) and 6-simply supported boundary condition is selected by the following implicit performance function whichis given based on the maximum displacement of the space truss structure in z-direction of the node under load $P1$ (Δ_{P1}^z) (Keshtegar and Kisi 2018)

$$g = 0.01 - |\Delta_{P1}^z| \tag{38}$$

The maximum displacement is computed based on Young's modulus of all bars (E), the section area of bars (A_i, i = 1, 2, 3,… 24) and the point loads (P_1 – P_7) whose statistical properties are listed in Table 4.

The converged results including numbers of iteration to compute the sensitivity vector (NI), numbers of call performance function to achieve the stabilization (NCF), converged reliability index (β) and absolute relative error of reliability index with MCS (RE %) of different reliability methods for Examples 1 and 2 are listed in Table 5. The results from Table 5 showed that the improved FORM algorithms including FSL, CHL-RF and RCR methods provide the stable results while the HL-RF and STM produce the unstable results as chaotic solutions for these two engineering reliability problems. The iHL-RF and

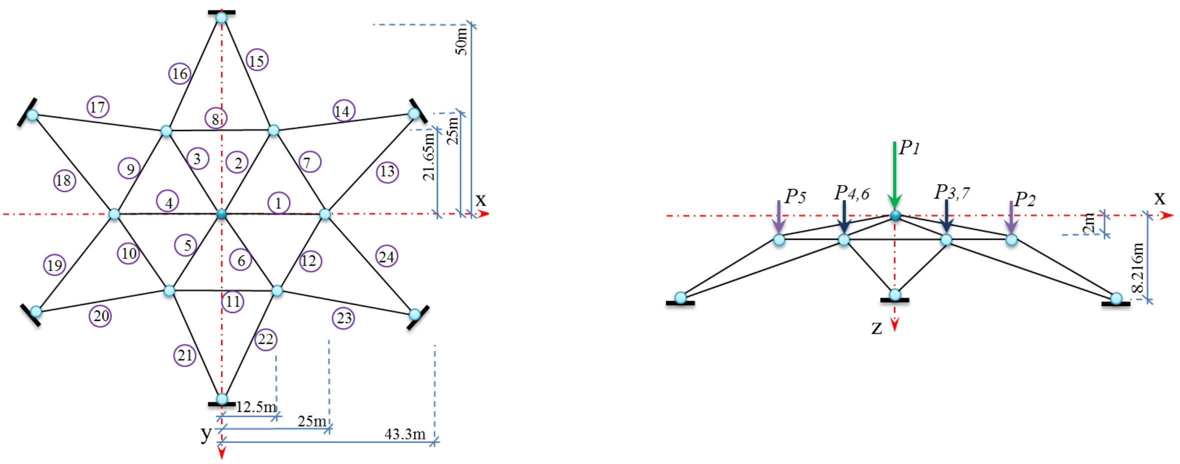

Fig. 4 Schematic view of 24-bar space truss example

Table 4 Random variables for space truss structure

Random variable	$A_1 - A_6$ (m^2)	$A_7 - A_{12}$ (m^2)	$A_{13} - A_{24}$ (m^2)	E (Gpa)	P_1 (kN)	$P_2 - P_7$ (kN)
Mean	0.013	0.01	0.016	205	20	10
CoV	0.1	0.1	0.1	0.12	0.15	0.12
Distribution	Normal	Normal	Normal	Normal	Gumbel	Gumbel

Table 5 The converged results of different reliability methods for Examples 1 and 2

Method	Example 1				Example 2			
	NCF	NI	β	RE%	NCF	NI	β	RE%
MCS	10^7	--	4.4163	--	6×10^5	--	1.7618	--
HL-RF	Not conversed		--		Not conversed			
STM (Yang 2010)	Not conversed		--		Not conversed			
FSL (Gong and Yi 2011)	2603	84	4.6280	4.79	4940	76	3.7390	112.23
iHL-RF (Liu and Der Kiureghian 1991)	5887	184	4.6278	4.79	Not conversed			
CHL-RF (Keshtegar and Miri 2014)	5517	178	4.6290	4.82	3965	61	1.6526	6.20
Proposed RCR	402	19	4.6276	4.78	3770	58	1.7354	1.50

CHL-RF are robustly converged about ten-time more computational burden than the proposed RCR method for Example 1 while the CHL-RF shows the same convergence property in terms of efficiency compared with RCR in Example 2 but it is more inaccurately. The FSL converges to stable results but it is significantly produced the inaccurate results compared to the conjugate FORM-based CHL-RF and RCR methods for Example 2. It is conducted from the results of Example 2, the conjugate search direction can be improve the FORM formula for both accuracy and robustness compared to the sensitivity analysis-based steepest descent search direction. Therefore, the search direction vector is an important factor in iterative FORM formula while the step size (control factor) is considerable factor in improved versions of FORM-based steepest descent search direction of *i*HL-RF, STM, and FSL methods. By improving the search direction based on the sufficient descent condition in conjugate selectivity vector, it is provided stable reliability results with accurate convergence, more efficiently.

5.3 Reliability analysis of nanocomposite beam

The converged results such as the reliability index, failure probability, number of evaluating performance function (NCF), number of iterations for computing gradient vector (NI) and the relative error of failure probability for different reliability methods with MCS (Rel-error %) are listed in Table 6.

Fig. 5 illustrates the histories of the reliability indexes for the STM, HL-RF, *i*HL-RF, FSL, CHL-RF and RCR methods, which are obtained based on the implicit limit state function in Eq. (31) of nanocomposite beam under buckling force. The results from the Table 6 and Fig. 5

Table 6 The converged results of different reliability methods for nanocomposite beam

Method	NCF	NI	Reliability index	Failure probability	Rel-error (P_f)%
MCS	2×10^{7}	--	3.1455	8.29×10^{-4}	--
HL-RF	Chaos	--	Not converged	--	N.A
STM (Yang 2010)	Chaos	--	Not converged	--	N.A
FSL (Gong and Yi 2011)	9661	69	3.126154	8.86×10^{-4}	-6.82
iHL-RF (Liu and Der Kiureghian 1991)	Chaos	--	Not converged	--	N.A
CHL-RF (Keshtegar and Miri 2014)	6124	46	3.122189	8.98×10^{-4}	-8.27
Proposed RCR	2993	27	3.138107	8.5×10^{-4}	-2.56

demonstrated that the proposed RCR method is converged to stable results, while the HL-RF, *i*HL-RF and STM are yielded unstable results as chaotic solutions. As seen, the search direction is an important issue as well as the step size (relaxed factor) to achieve the stabilization. The conjugate search direction may provide the normalized vector to compute the new point, which is not located along the previous steepest descent search direction vector. Thus, it may reduce the parallel risk of the sequential normalized vectors. It can be conducted from the results of Table 3 and Fig. 3 that the two conjugate FORM algorithms i.e., CHL-RF and RCR are yielded to stable results compared to the HL-RF, *i*HL-RF and STM formulas, which are formulated using steepest descent search direction. The reliability methods based on HL-RF, *i*HL-RF and STM (see Eqs. (32) -(34)) produce the unstable results for this problem, while the FSL, CHL-RF and RCR can be enriched the robustness of the FORM formula using modified search direction by finite-step size for reliability analysis of this practical engineering nanocomposite problem. The finite-step size in FSL and CHL-RF is adjusted by the condition $\|\boldsymbol{U}_{k+1}-\boldsymbol{U}_k\| \geq \|\boldsymbol{U}_k-\boldsymbol{U}_{k-1}\|$ that this limited criterion is also applied to adjust the relaxed factor in the proposed method based on Eq. (13). Consequently, the search direction in FSL and CHL-RF using finite-step size and the new point in proposed RCR method based on relaxed factor is adjusted by using the condition $\|\boldsymbol{U}_{k+1}-\boldsymbol{U}_k\| \geq \|\boldsymbol{U}_k-\boldsymbol{U}_{k-1}\|$, thus it can be conducted that $\lambda_{k+1} < \lambda_k$ for highly nonlinear problems. Thus, the step size or (relaxed factor) is followed to zero when $\|\boldsymbol{U}_{k+1}-\boldsymbol{U}_k\| \geq \|\boldsymbol{U}_k-\boldsymbol{U}_{k-1}\|$ for $k \to \infty$. Consequently, it is provided the stable results using the FSL, CHL-RF and proposed RCR methods that it can be extracted from the results of Table 6 and Fig. 5.

The CHL-RF and FSL are as robust as the RCR method but are more inefficient and inaccurate. The RCR method is converged about three times less number of evaluating the LSF than the FSL to reliability index of 3.138107 and MPP

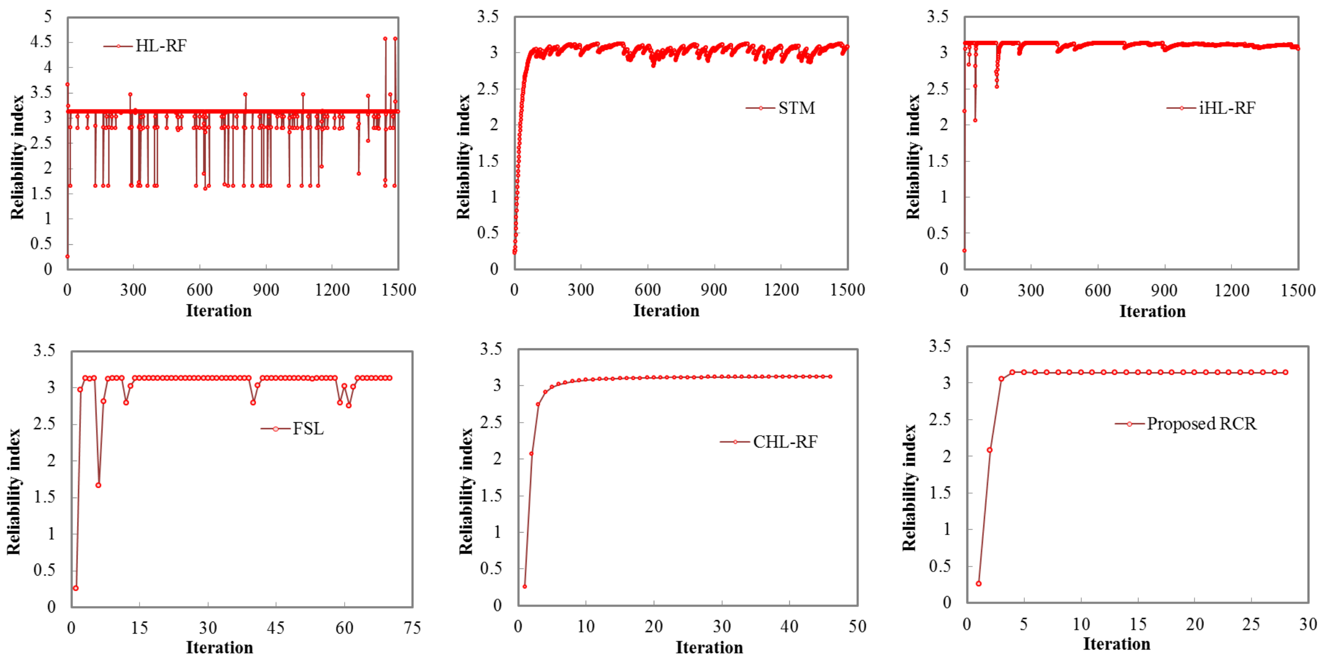

Fig. 5 The convergence reliability index histories of different reliability methods for nanocomposite beam

Table 7 The converged results of RSM-based MCS and RCR for nanocomposite beam

Method	NCF	Reliability index	Failure probability	Rel-error (P_f)%
RSM-MCS	100	3.2605	5.56×10^{-4}	32.92
	500	3.2249	6.31×10^{-4}	23.99
	1000	3.1899	7.12×10^{-4}	14.16
	2000	3.1792	7.38×10^{-4}	10.93
RSM-RCR	100	3.2903	5.10×10^{-4}	39.64
	500	3.2770	5.25×10^{-4}	36.72
	1000	3.1861	7.21×10^{-4}	13.02
	2000	3.1165	9.15×10^{-4}	-10.37

of (h = 0.39659 (m), L = 0.374741 (m), k_w = 4.4352×10^{12} (N/m^2), k_g = 4.899567 (N), rho = 0.248509, V_0 = 100.5096 (volte)) after 27 iterations.

The response surface method (RSM) is applied to give the predicted limit sate function that this methodology may improve the accuracy and efficiency with simple relation of the implicit limit state function in Eq. (33). The RSM combined by the MCS (RSM+MCS) and proposed RCR (RSM+RCR) is also applied to demonstrate the improvement of the convergence performance of nonlinear reliability problem, which is extracted by the applicable engineering nanocomposite beam in this section. The results of reliability analyses for different training samples i.e., 100, 500, 1000 and 2000 data points which are utilized to build the second-order polynomial function with crossterms are presented in Table 7 for RSM + MCS and RSM + RCR methods. As seen from Table 7, by increasing the training sample point for both RSM combined by MCS and RCR methods; the reliability results are improved for accuracy predictions. The efficiency of this reliability problem in terms of computational burden of limit state function is strongly improved compared to the analytical reliability models. The CRC provides stable results for different training samples (NCF) in RSM with an acceptable

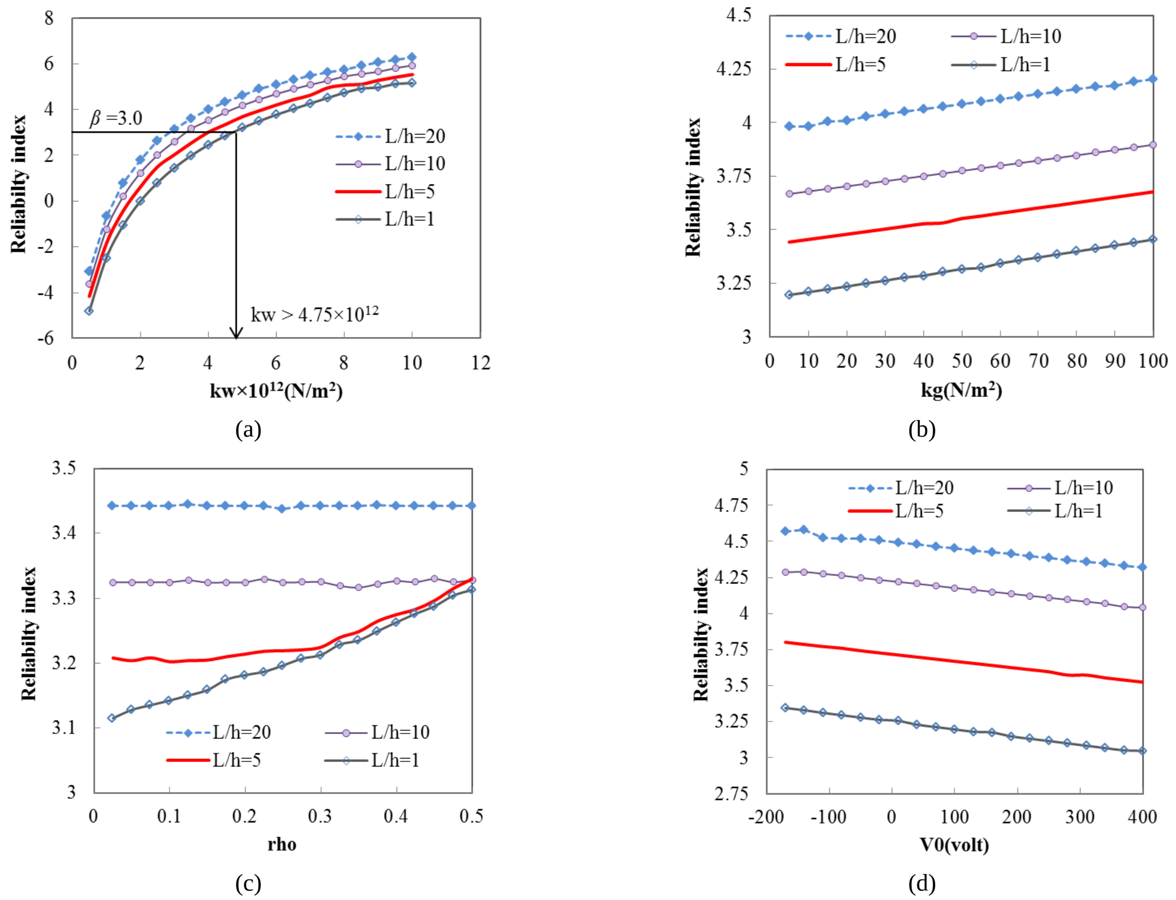

Fig. 6 Effects of the length to thickness on the reliability index of beam versus (a) spring constant of foundation; (b) shear constant of foundation; (c) ZnO volume percent; (d) external applied voltage

reliability index for this complex problem. It can be conducted that the surrogate models-based analytical approaches can be strongly improved the efficiency of the implicit performance function in studied nanocomposite beam.

The reliability indexes corresponding to the various means of variables including spring constant of foundation (k_w), shear constant of foundation (k_g), volume fraction of ZnO nanoparticle (*rho*), and applied voltage (V_0) for different length to thickness ratio are shown in Figs. 6(a)-(d), respectively. The reliability indexes for nanocomposite beam under buckling failure mode are determined based on the proposed RCR method. The comparative results are obtained based on the basic random variables in Table 1 with constant coefficients of variation and distribution functions. As seen, the reliability indexes are increased by increasing the input random variables k_w, *rho*, and k_g, while are decreasing with respect to increasing the voltage. The increasing rate of the reliability index are significantly shown for k_w compared to other random variable in the almost length to thickness ratio of beam. By increasing the length to thickness ratio, the reliability indexes are increased for all cases. It can be concluded that the reliability index (failure probability of beam) is significantly sensitive to the spring constant of foundation, while failure probability of beam is insensitive to *rho* in compassion with other basic random variable. The reliability indexes are obtained more than 3 for k_w > 4.75×10^{12}(N/m^2), k_g > 0, *rho* > 0 and V_0 < 400 volts. Therefore, a good confidence level (e.g., the failure probability less than $P_f = 1.35\times10^{-3}$) can be obtained for nanocomposite beams based on conditions $k_w > 4.75\times10^{12}$ N/m^2 and V_0 < 400 volt.

Fig. 7 illustrates the effects of the mode number (mm) of buckling on the reliability index of beam. It can be conducted that the confidence level of the beam is slightly increasing with respect to the mm < 4 for all length to thickness ratio. For L/h = 1, the reliability index can be obtained more than 3 when the mode number of bucking force is given more than 14 for this beam.

The effects of the volume fractions of ZnO nano-particles on the reliability index for different spring constants of foundation (k_w with the means of 5, 5.5, 6 and 6.5 $\times10^{12}$ N/m^2), shear constants of foundation (k_g with the means of 0, 10, 20, 30 N) and applied voltages (V_0 with the means of -200, -100, 100, 200 volte) are shown in Fig. 8(a)-(c), respectively. It can be concluded that increasing the volume fraction of ZnO nanoparticles leads to increase in the reliability index. It is due to the fact that increasing the volume fraction of ZnO nanoparticles makes the structure stiffer. In addition, increasing the spring and shear constant of elastic medium makes the structure stiffer and consequently higher reliability index. Furthermore, applying negative external voltage induced a compressive load to the structure and consequently, the reliability index increases. Noted that the mentioned phenomenon for positive external voltage in converse.

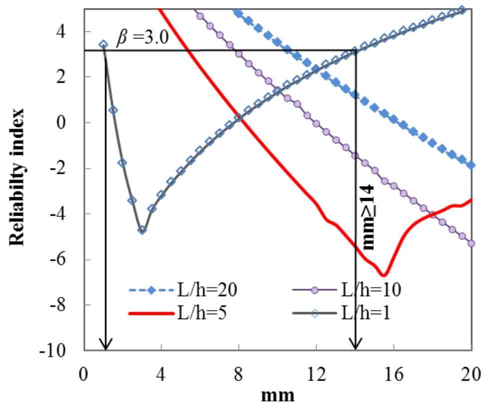

Fig. 7 Effects of the mode number of buckling on the reliability index of beam

6. Conclusions

The first-order reliability method (FORM) is enriched based on the conjugate search direction-based relaxed approach to achieve accurate and stable reliability analysis of nanocomposite beam under buckling performance function. The proposed relaxed conjugate reliability method (RCR) are formulated using an adjusted relaxed factor and limited conjugate scalar factor. The results of RCR method for a reinforced nanocomposite beam under buckling implicit limit state function is compared with the existing reliability methods including HL-RF, improved HL-RF, stability transformation method (STM), the finite-step length (FSL) and conjugate HL-RF. The ZnO nanoparticles-reinforced beam is simulated by SSDT that the critical

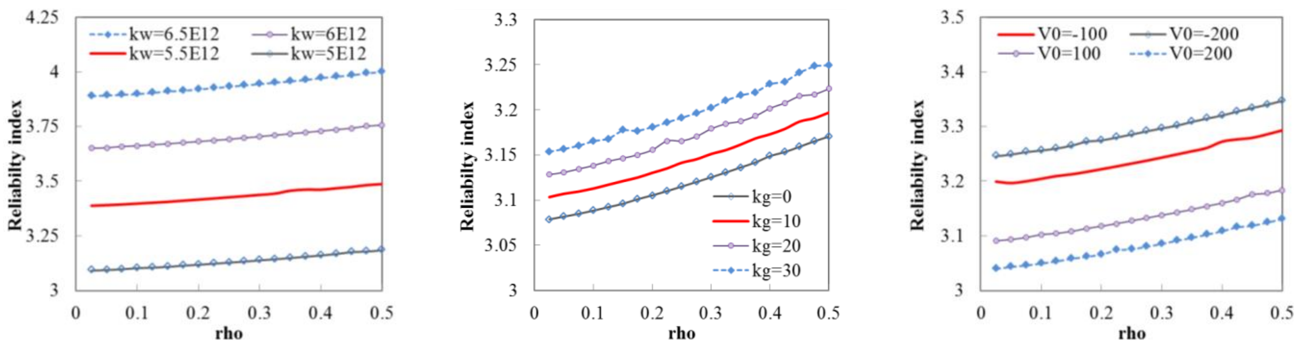

Fig. 8 Effects of the volume fraction of ZnO nanoparticles on the reliability index of nanocomposite beam for different (a) spring constant of foundation; (b) shear constant of foundation; (c) ZnO volume percent

buckling loads of nanocomposite beam are calculated using an analytical solution. The reliability results of the buckling failure mode for nanocomposite beams showed that the RCR method is more accurate and efficient than the CHL-RF and FSL methods while is more robust than HL-RF, STM, and iHL-RF. The proposed RCR is efficient and robust approach, thus the RCR method can be applied for evaluating the failure probabilities of nanocomposite structures, the reliability problems with correlated random variables, highly nonlinear and high-dimensional applicable reliability problems, reliability in future.

The proposed RCR method is applied to reliability analysis of nanocomposite beam that good confidence levels (reliability index more than 3) can be obtained when spring constant of foundation more than 4.75×10^{12} (N/m^2) and applied voltage less than 400 volets. Furthermore, reliability index is increased by increasing the volume fraction of ZnO nanoparticles. In addition, applying negative voltage makes the structure stiffer and leads to higher reliability index.

References

Alibrandi, U., Alani, A.M. and Ricciardi, G. (2015), "A new sampling strategy for SVM-based response surface for structural reliability analysis", *Probabil. Eng. Mech.*, **41**, 1-12.

Averseng, J., Bouchair, A. and Chateauneuf, A. (2017), "Reliability analysis of the nonlinear behaviour of stainless steel cover-plate joints", *Steel Compos. Struct., Int. J.*, **25**(1), 45-55.

Barzoki, A., Mosallaie, A., Ghorbanpour Arani, A., Kolahchi, R. and Mozdianfard, M.R. (2012), "Electro-thermo-mechanical torsional buckling of a piezoelectric polymeric cylindrical shell reinforced by DWBNNTs with an elastic core", *Appl. Math. Model.*, **36**(1), 2983-2995.

Bonstrom, H. and Corotis, R.B. (2014), "First-order reliability approach to quantify and improve building portfolio resilience", *J. Struct. Eng.*, **142**(8), p.C4014001.

Chojaczyk, A.A., Teixeira, A.P., Neves, L.C., Cardoso, J.B. and Guedes Soares, C. (2015), "Review and application of artificial neural networks models in reliability analysis of steel structures", *Struct. Safe.*, **52**, 78-89.

Der Kiureghian, A. and Dakessian, T. (1998), "Multiple design points in first and second-order reliability", *Struct. Safe.*, **20**(1), 37-49.

Dubourg, V., Sudret, B. and Bourinet, J.M. (2011), "Reliability-based design optimization using kriging surrogates and subset simulation", *Struct. Multidiscipl. Optimiz.*, **44**(5), 673-690.

Duc, N.D., Hadavinia, H., Van Thu, P. and Quan, T.Q. (2015), "Vibration and nonlinear dynamic response of imperfect three-phase polymer nanocomposite panel resting on elastic foundations under hydrodynamic loads", *Compos. Struct.*, **131**, 229-237.

Duc, N.D., Cong, P.H., Tuan, N.D., Tran, P. and Van Thanh, N. (2017a), "Thermal and mechanical stability of functionally graded carbon nanotubes (FG CNT)-reinforced composite truncated conical shells surrounded by the elastic foundation", *Thin-Wall. Struct.*, **115**, 300-310.

Duc, N.D., Lee, J., Nguyen-Thoi, T. and Thang, P.T. (2017b), "Static response and free vibration of functionally graded carbon nanotube-reinforced composite rectangular plates resting on Winkler–Pasternak elastic foundations", *Aerosp. Sci. Technol.*, **68**, 391-402.

Duc, N.D., Tran, Q.Q. and Nguyen, D.K. (2017c), "New approach to investigate nonlinear dynamic response and vibration of imperfect functionally graded carbon nanotube reinforced composite double curved shallow shells subjected to blast load and temperature", *Aerosp. Sci. Technol.*, **71**, 360-372.

Duc, N.D., Seung-Eock, K., Quan, T.Q., Long, D.D. and Anh, V.M. (2018), "Nonlinear dynamic response and vibration of nanocomposite multilayer organic solar cell", *Compos. Struct.*, **184**, 1137-1144.

Echard, B., Gayton, N. and Lemaire, M. (2011), "AK-MCS: An active learning reliability method combining Kriging and Monte Carlo Simulation", *Struct. Safe.*, **33**(2), 145-154.

Echard, B., Gayton, N., Lemaire, M. and Relun, N. (2013), "A combined importance sampling and kriging reliability method for small failure probabilities with time-demanding numerical models", *Reliabil. Eng. Syst. Safe.*, **111**, 232-240.

El Amine Ben Seghier, M., Keshtegar, B. and Bouali, E. (2018), "Reliability analysis of low, mid and high-grade strength corroded pipes based on plastic flow theory using adaptive nonlinear conjugate map", *Eng. Fail. Anal.*, **90**, 245-246.

Ghorbanpour, A., Abdollahian, M. and Kolahchi, R. (2015), "Nonlinear vibration of embedded smart composite microtube conveying fluid based on modified couple stress theory", *Polym. Compos.*, **36**(7), 1314-1324.

Gong, J.X. and Yi, P. (2011), "A robust iterative algorithm for structural reliability analysis", *Struct. Multidiscipl. Optimiz.*, **43**(4), 519-527.

Goswami, S., Ghosh, S. and Chakraborty, S. (2016), "Re Reliability analysis of structures by iterative improved response surface method", *Struct. Safe.*, **60**, 56-66.

Hasofer, A.M. and Lind, N.C. (1974), "Exact and invariant second-moment code format", *J. Eng. Mech. Div.*, **100**(1), 111-121.

Hu, C. and Youn, B.D. (2011), "Adaptive-sparse polynomial chaos expansion for reliability analysis and design of complex engineering systems", *Struct. Multidiscipl. Optimiz.*, **43**(3), 419-442.

Jia, B., Yu, X.L. and Yan, Q.S. (2016), "A new sampling strategy for Kriging-based response surface method and its application in structural reliability", *Adv. Struct. Eng.*, **20**(4), 564-581.

Keshtegar, B. (2016), "Chaotic conjugate stability transformation method for structural reliability analysis", *Comput. Methods Appl. Mech. Eng.*, **310**, 866-885.

Keshtegar, B. (2017), "Limited conjugate gradient method for structural reliability analysis", *Eng. Comput.*, **33**(3), 621-629.

Keshtegar, B. (2018a), "Enriched FR conjugate search directions for robust and efficient structural reliability analysis", *Eng. Comput.*, **34**(1), 117-128.

Keshtegar, B. (2018b), "Conjugate finite-step length method for efficient and robust structural reliability analysis", *Struct. Eng. Mech., Int. J.*, **65**(4), 415-422.

Keshtegar, B. and Bagheri, M. (2018), "Fuzzy relaxed-finite step size method to enhance the instability of the fuzzy first-order reliability method using conjugate discrete map", *Nonlinear Dyn.*, **91**(3), 1443-1459.

Keshtegar, B. and Chakraborty, S. (2018a), "An efficient -robust structural reliability method by adaptive finite-step length based on Armijo line search", *Reliabil. Eng. Syst. Safe.*, **172**, 195-206.

Keshtegar, B. and Chakraborty, S. (2018b), "A hybrid self-adaptive conjugate first order reliability method for robust structural reliability analysis", *Appl. Math. Model.*, **53**, 319-332.

Keshtegar, B. and Kisi, O. (2017), "M5 model tree and Monte Carlo simulation for efficient structural reliability analysis", *Appl. Math. Model.*, **48**, 899-910.

Keshtegar, B. and Meng, Z. (2017), "A hybrid relaxed first-order reliability method for efficient structural reliability analysis", *Struct. Safe.*, **66**, 84-93.

Keshtegar, B. and Miri, M. (2014), "Reliability analysis of corroded pipes using conjugate HL–RF algorithm based on average shear stress yield criterion", *Eng. Fail. Anal.*, **46**, 104-117.

Kolahchi, R., Bidgoli, M.R., Beygipoor, G. and Fakhar, M.H. (2015), "A nonlocal nonlinear analysis for buckling in embedded FG-SWCNT-reinforced microplates subjected to magnetic field", *J. Mech. Sci. Technol.*, **29**(9), 3669-3677.

Kolahchi, R., Hosseini, H. and Esmailpour, M. (2016), "Differential cubature and quadrature-Bolotin methods for dynamic stability of embedded piezoelectric nanoplates based on visco-nonlocal-piezoelasticity theories", *Compos. Struct.*, **157**, 174-186.

Lee, T.H. and Jung, J.J. (2008), "A sampling technique enhancing accuracy and efficiency of metamodel-based RBDO: Constraint boundary sampling", *Comput. Struct.*, **86**(13), 1463-1476.

Lee, I., Choi, K.K., Du, L. and Gorsich, D. (2008), "Dimension reduction method for reliability-based robust design optimization", *Comput. Struct.*, **86**(13-14), 1550-1562.

Li, C., Zhang, Y., Tu, W., Jun, C., Liang, H. and Yu, H. (2017), "Soft measurement of wood defects based on LDA feature fusion and compressed sensor images", *J. Forest. Res.*, **28**(6), 1285-1292.

Liu, P.L. and Der Kiureghian, A. (1991), "Optimization algorithms for structural reliability", *Struct. Safe.*, **9**(3), 161-177.

Liu, Y.W. and Moses, F. (1994), "A sequential response surface method and its application in the reliability analysis of aircraft structural systems", *Struct. Safe.*, **16**(1-2), 39-46.

Lu, Z.H., Zhao, Y.G., Yu, Z.W. and Chen, C. (2015), "Reliability-based assessment of American and European specifications for square CFT stub columns", *Steel Compos. Struct., Int. J.*, **19**(4), 811-827.

Lu, Z.H., Cai, C.H. and Zhao, Y.G. (2017), "Structural reliability analysis including correlated random variables based on third-moment transformation", *J. Struct. Eng.*, **143**(8), p.04017067.

Meng, Z., Li, G., Yang, D. and Zhan, L. (2017), "A new directional stability transformation method of chaos control for first order reliability analysis", *Struct. Multidiscipl. Optimiz.*, **55**(2), 601-612.

Mosharrafian, F. and Kolahchi, R. (2016), "Nanotechnology, smartness and orthotropic nonhomogeneous elastic medium effects on buckling of piezoelectric pipes", *Struct. Eng. Mech., Int. J.*, **58**(5), 931-947.

Rackwitz, R. and Flessler, B. (1978), "Structural reliability under combined random load sequences", *Comput. Struct.*, **9**(5), 489-494.

Shen, H.S. (2009), "Nonlinear bending of functionally graded carbon nanotube-reinforced composite plates in thermal environments", *Compos. Struct.*, **91**(1), 9-19.

Shen, H.S. and Zhang, C.L. (2010), "Thermal buckling and postbuckling behavior of functionally graded carbon nanotube-reinforced composite plates", *Mater. Des.*, **31**(7), 3403-3411.

Song, M., Yang, J., Kitipornchai, S. and Zhu, W. (2017), "Buckling and postbuckling of biaxially compressed functionally graded multilayer graphene nanoplatelet-reinforced polymer composite plates", *Int. J. Mech. Sci.*, **131-~~132~~**, 345-355.

Tan, P. and Tong, L. (2001), "Micro-electromechanics models for piezoelectric-fiber-reinforced composite materials", *Compos. Sci. Technol.*, **61**(5), 759-769.

Tagrara, S.H., Benachour, A., Bouiadjra, M.B. and Tounsi, A. (2015), "On bending, buckling and vibration responses of functionally graded carbon nanotube-reinforced composite beams", *Steel Compos. Struct., Int. J.*, **19**(5), 1259-1277.

Thai, H.T. and Vo, T.P. (2012), "A nonlocal sinusoidal shear deformation beam theory with application to bending, buckling, and vibration of nanobeams", *Int. J. Eng. Sci.*, **54**(1), 58-66.

Thanh, N.V., Khoa, N.D., Tuan, N.D., Tran, P. and Duc, N.D. (2017), "Nonlinear dynamic response and vibration of functionally graded carbon nanotube-reinforced composite (FG-CNTRC) shear deformable plates with temperature-dependent material properties", *J. Therm. Stress.*, **40**(10), 1254-1274.

Van Thu, P. and Duc, N.D. (2016), "Non-linear dynamic response and vibration of an imperfect three-phase laminated nanocomposite cylindrical panel resting on elastic foundations in thermal environment", *Sci. Eng. Compos. Mater.*, **24**(6), 951-962.

Vodenitcharova, T. and Zhang, L.C. (2006), "Bending and local buckling of a nanocomposite beam reinforced by a single-walled carbon nanotube", *Int. J. Solid. Struct.*, **43**(10), 3006-3024.

Wattanasakulpong, N. and Ungbhakorn, V. (2013), "Analytical solutions for bending, buckling and vibration responses of carbon nanotube-reinforced composite beams resting on elastic foundation", *Computat. Mater. Sci.*, **71**, 201-208.

Wuite, J. and Adali, S. (2005), "Deflection and stress behaviour of nanocomposite reinforced beams using a multiscale analysis", *Compos. Struct.*, **71**(3-4), 388-396.

Yang, D. (2010), "Chaos control for numerical instability of first order reliability method", *Commun. Nonlinear Sci. Numer. Simul.*, **15**(10), 3131-3141.

Yang, H. and Yu, L. (2017), "Feature extraction of wood-hole defects using wavelet-based ultrasonic testing", *J. Forest. Res.*, **28**(2), 395-402.

Zhao, Y.G. and Lu, Z.H. (2007), "Fourth-moment standardization for structural reliability assessment", *J. Struct. Eng.*, **133**(7), 916-924.

Zhao, Y.G. and Ono, T. (2001), "Moment methods for structural reliability", *Struct. Safe.*, **23**(1), 47-75.

Zhou, W., Li, S., Jiang, L. and Huang, Z. (2015), "Distortional buckling calculation method of steel-concrete composite box beam in negative moment area", *Steel Compos. Struct., Int. J.*, **19**(5), 1203-1219.

Zhuang, X. and Pan, R. (2012), "A sequential sampling strategy to improve reliability-based design optimization with implicit constraint functions", *J. Mech. Des.*, **134**(2), 021002.

CC